Various Processes in the Converter Resonant Tank Circuits

Aleksandar Vuchev[1], Nikolay Bankov[2], Yasen Madankov[3] and Angel Lichev[4]

[1]Aleksandar Vuchev is with the Department of Electrical
Engineering and Electronics, Technical Faculty, University of Food
Technologies, 26 Maritza Blvd., 4002 Plovdiv, Bulgaria
avuchev@yahoo.com

[2]Nikolay Bankov is with the Department of Electrical Engineering
and Electronics, Technical Faculty, University of Food
Technologies, 26 Maritza Blvd., 4002 Plovdiv, Bulgaria
nikolay_bankov@yahoo.com

[3]Yasen Madankov is with the Department of Electrical
Engineering and Electronics, Technical Faculty, University of Food
Technologies, 26 Maritza Blvd., 4002 Plovdiv, Bulgaria
yasen.madankov@gmail.com

[4]Angel Lichev is with the Department of Electrical Engineering
and Electronics, Technical Faculty, University of Food
Technologies, 26 Maritza Blvd., 4002 Plovdiv, Bulgaria
angel_lichev@abv.bg

ABSTRACT: *In this work, we have addressed the bidirectional series resonant DC-DC converter which has more resonant frequency. We have also described the conditions of operation with ZV. The processes in the converter resonant tank circuit are presented on the basis of well-known analytical models and their coefficients are defined. We have conducted experiments where the theoretical results are compared with those from simulation in the environment.*

I. Introduction

The bidirectional DC-DC converters are suitable for different applications where it is necessary to control the electrical energy transmission [3], such as in motor drives [4, 8], grids with renewable energy sources [6, 9], etc. They are realized on the base of two inverter stages. For connection between the inverters, a single inductance can be used [5, 9].

It is long known that series resonant DC-DC converters can also be used for bidirectional energy transfer [1, 3, 4]. They have various advantages, one of which is the possibility of significant switching loss reduction. When the converters operate above the resonant frequency, it is really possible that their power devices switch at zero voltage (ZVS – Zero Voltage Switching) [2]. This makes them a preferred solution for different applications.

There is a plenty of investigations [3, 4, 7, 10] of bidirectional series resonant DC-DC converters operating at higher than their resonant frequency. They show that the characteristics of the considered solutions depend on the applied control technique to a significant extend. It is known that these characteristics can be obtained as a result of modelling of the converter resonant tank circuit processes [2]. In general, this is the description of the variation of the inductor current and the capacitor voltage. These models are well-known, but their coefficients depend on the converter circuit and the used control technique.

The current work presents analytical modelling of the resonant tank circuit processes of bidirectional series resonant DC-DC converter operating above the resonant frequency. For this purpose, well-known analytical models are used and their coefficients are determined for the considered circuit.

2. Principle of the Converter Operation

Circuit of the examined converter is presented in Figure 1. It consists of two identical bridge inverter stages, resonant tank circuit (L, C), matching transformer T_r, capacitive input and output filters $(C_d$ и $C_0)$. Figure 1 also presents the snubber capacitors $C_1 \div C_8$ by which a zero voltage switching is obtained.

A voltage U_d is applied to the DC terminals of the "input" inverter stage (transistors $Q_1 \div Q_4$ with freewheeling diodes $D_1 \div D_4$), and a voltage U_0 – to those of the "output" stage (transistors $Q_5 \div Q_8$ with freewheeling diodes $D_5 \div D_8$).

Depending on the energy transfer direction, two operating modes are possible for the converter. The first of them is called DIRECT MODE. In this mode, it is assumed that energy flows from the "input" to the "output", i.e. from the source of voltage U_d to the one of voltage U_0. The second is REVERCE MODE. In this mode, the energy flows from the
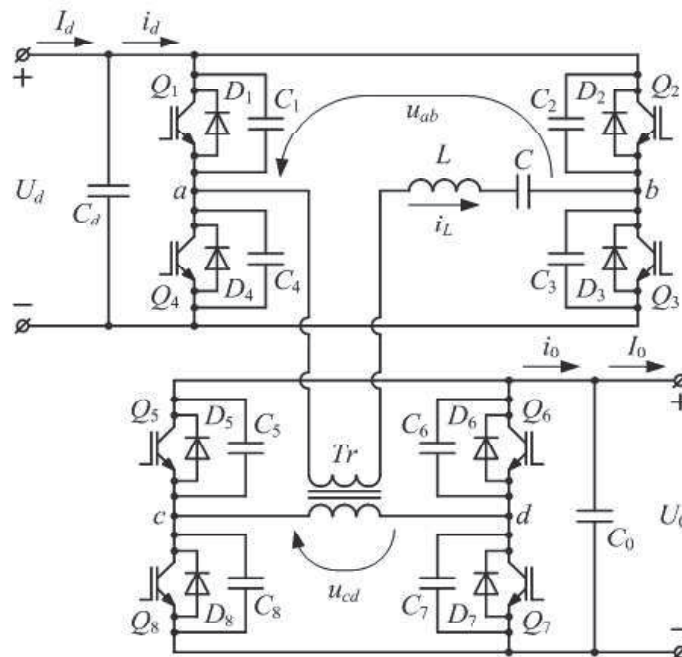

Figure 1. Circuit of the Bidirectional Resonant DC/DC Converter

"output" to the "input" (from U_0 to U_d). The waveforms, shown in Figure 2, illustrate the converter operation in DIRECT MODE, and those in Figure 3 – in REVERCE MODE.

Independently from the mode, the converter operates at constant frequency ω_s, which is higher than the resonant ω_0. Therefore, the transistor pairs of the "input" stage $(Q_1, Q_3$ or $Q_2, Q_4)$ operate at ZVS. They are controlled in such way that the voltage uab
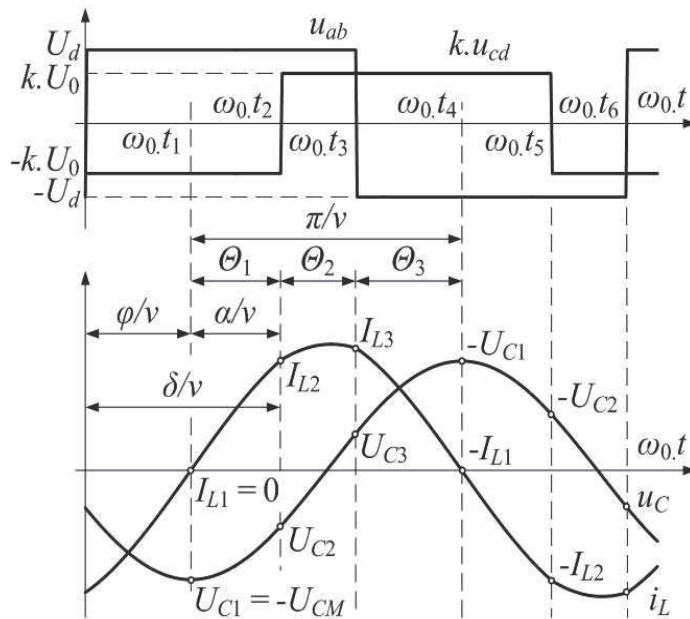
Figure 2. Waveforms at DIRECT MODE

has almost square-wave form and amplitude U_d. Along with this, the resonant current i falls behind the voltage uab at an angle φ. The transistors of the "output" stage also operate at ZVS. Therefore, when the current i passes through zero, the corresponding pair (Q_5, Q_7 or Q_6, Q_8) begins conducting. This pair switches off after time, corresponding to an angle δ, accounted to the moment of switch-off of the "input" stage transistors that conducted in the same half cycle. The voltage u_{cd}, which also has almost square-wave form and amplitude δ, which also has almost square-wave form and amplitude U_d, is shifted in time from u_{ab}. In this way, the output power control is obtained by phase-shifting – the variation of the angle δ.

Angle φ corresponds to the conduction time of the "input" stage freewheeling diodes, and angle α – to the conduction time of the "output" stage transistors. When φ < π/2 and α < π/2, energy is transferred in "forward" direction, and when φ > π/2 and α > π / 2 – in "reverse" direction. From Figures 2 and 3, it can be observed that the following equation is valid: φ + α. δ Therefore, when δ < π, REVERCE MODE is observed, and when δ < π – DIRECT MODE.

Angles φ, α and δ are related to the operating frequency $ω_S$.

3. Modeling of the Converter Operation

For the purposes of the analysis, the following assumptions are made: the matching transformer is ideal with a transformation ratio k, all the circuit elements are ideal, the influence of the snubber capacitors $C_1 ÷ C_8$ and the ripples of the "input" voltage U_d and the "output" voltage U_0 are neglected, i.e. voltages u_{ab} and u_{cd} have rectangular shape.

The waveforms (Figures 2 and 3) show that, independently from the converter mode, any of the half cycles can be divided into three intervals. For each of them, an equivalent DC voltage U_{EQ}, defined by the values of uab and ucd, is applied to the resonant tank circuit. This fact allows only the resonant tank circuit processes to be investigated. Therefore, apart from the waveforms of the current i_L through the inductor L and the voltage u_C across the capacitor C, Figsures 2 and 3 show the initial values ($I_{L1} ÷ I_{L1'}$, $U_{C1} ÷ U_{C3}$) for each of the mentioned intervals.

In accordance with the assumptions made, the resonant frequency, the characteristic impedance and the frequency detuning are:
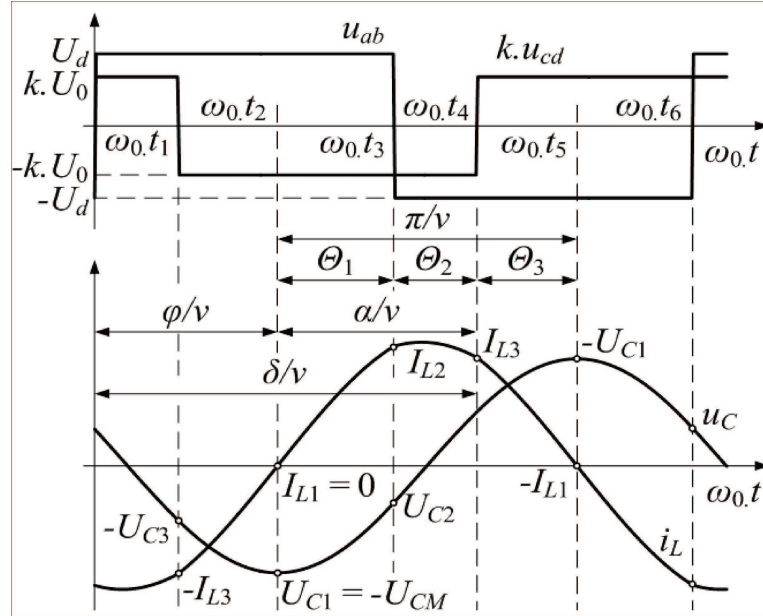
Figure 3. Waveforms at REVERCE MODE

$$\omega_0 = 1/\sqrt{LC}\ ;\ \rho_0 = \sqrt{L/C};\ \nu = \omega_S / \omega_0 \tag{1}$$

Because of the similarity, the modelling of the resonant tank circuit processes is realized in the same way as in [2]. For each of the half cycle intervals, the current i_L and the voltage u_C values are determined as follows:

$$i_{Lj}(\theta) = I_{Lj} \cos\theta - \frac{U_{Cj} - U_{EQ_j}}{\rho_0} \sin\theta$$
$$u_{Cj}(\theta) = \rho_0 I_{Lj} \sin\theta + \left(U_{Cj} - U_{EQ_j}\right)\cos\theta + U_{EQ_j} \tag{2}$$

where j is the number of the considered interval; I_{Lj} and U_{Cj} are the inductor current and the capacitor voltage values at the beginning of the interval; $\theta = 0 \div \Theta_j$; Θ_j – angle of the interval or the resonant frequency ω_0; U_{EQj} – the value of the equivalent DC voltage applied to the resonant tank circuit.

Actually, the parameters I_{Lj}, U_{Cj} и U_{EQj} represent coefficients of the modelling Eqs. (2).

In order to obtain generalized results, all the quantities are normalized as follows: the voltages according to U_d; and the currents – according to U_d/ρ_0. Then, Eqs. (2) are transformed and in normalized form are:

$$i'_{Lj}(\theta) = I'_{Lj} \cos\theta - \left(U'_{Cj} - U'_{EQ_j}\right)\sin\theta$$
$$u'_{Cj}(\theta) = I'_{Lj} \sin\theta + \left(U'_{Cj} - U'_{EQ_j}\right)\cos\theta + U'_{EQ_j} \tag{3}$$

where the normalized values of the corresponding quantities are marked with the prime symbol.

From Figures 2 and 3 it is observed that the value of i_L at the end of given interval appears to be initial value for the following one. The same applies to the voltage u_C. Therefore:

$$I'_{Lj+1} = I'_{Lj}\cos\Theta_j - \left(U'_{Cj} - U'_{EQ_j}\right)\sin\Theta_j$$
$$U'_{Cj+1} = I'_{Lj}\sin\Theta_j + \left(U'_{Cj} - U'_{EQ_j}\right)\cos\Theta_j + U'_{EQ_j} \tag{4}$$

Taking into consideration that $I_{L3} = -I_{L1}$ and $U_{C3} = -I_{L3}$, after recursion of the Eqs. (4) the following system is obtained for the three consecutive intervals in a half cycle:

$$I'_{L1}\left(1 + \cos\frac{\pi}{\nu}\right) - U'_{C1}\sin\frac{\pi}{\nu}$$

$$= \sum_{j=1}^{3} U'_{EQ_j}\left[\sin\left(\frac{\pi}{\nu} - \sum_{i=1}^{j}\Theta_i\right) - \sin\left(\sum_{i=j}^{3}\Theta_i\right)\right] \tag{5}$$

$$I'_{L1}\sin\frac{\pi}{\nu} + U'_{C1}\left(1 + \cos\frac{\pi}{\nu}\right)$$

$$= \sum_{j=1}^{3} U'_{EQ_j}\left[\cos\left(\sum_{i=j}^{3}\Theta_i\right) - \cos\left(\frac{\pi}{\nu} - \sum_{i=1}^{j}\Theta_i\right)\right] \tag{6}$$

It is convenient the interval at which the initial values are $I_{L1} = 0$ and $U_C = -U_{CM}$ to be chosen as first. In this case, the parameters Θ_j and U'_{EQj} are defined on the base of the waveforms (Figures 2 and 3). Their values are presented in Table 1 for each of the two operating modes.

As $I'_{L1} = 0$, after substitution of the actual values for U'_{EQj} in Eqs. (5) and (6), expressions for the voltages U'_0 and U'_{CM} are obtained. Thus, for the DIRECT MODE the following normalized dependencies are obtained:

MODE	Parameter	Number of interval		
		1	2	3
DIRECT	Θ_j	$\dfrac{\delta - \varphi}{\nu}$	$\dfrac{\pi - \delta}{\nu}$	$\dfrac{\varphi}{\nu}$
	U'_{EQj}	$1 + kU'_0$	$1 - kU'_0$	$-1 - kU'_0$
REVERCE	Θ_j	$\dfrac{\pi - \varphi}{\nu}$	$\dfrac{\delta - \pi}{\nu}$	$\dfrac{\pi - \delta + \varphi}{\nu}$
	U'_{EQj}	$1 + kU'_0$	$-1 + kU'_0$	$-1 - kU'_0$

Table 1

$$U'_0 = \frac{1}{k}\frac{\sin(\Theta_1 + \Theta_2) - \sin(\Theta_3)}{\sin(\Theta_2 + \Theta_3) - \sin(\Theta_1)} \tag{7}$$

$$U'_{CM} = 2\frac{\sin(\Theta_3) + U'_0\sin(\Theta_2 + \Theta_3)}{\sin(\pi/\nu)} - \left(1 + kU'_0\right) \tag{8}$$

Respectively, for the REVERCE MODE the following is obtained:

$$U'_0 = \frac{1}{k}\frac{\sin(\Theta_1) - \sin(\Theta_2 + \Theta_3)}{\sin(\Theta_3) - \sin(\Theta_1 + \Theta_2)} \tag{9}$$

$$U'_{CM} = 2\frac{\sin(\Theta_2 + \Theta_3) + U'_0 \sin(\Theta_3)}{\sin(\pi/\nu)} - (1 + kU'_0) \qquad (10)$$

When the values for the angles Θ_j are substituted in the above equations, identical expressions are obtained for the two operating modes:

$$U'_0 = \frac{1}{k}\frac{\sin\left(\dfrac{\pi - \varphi}{\nu}\right) - \sin\left(\dfrac{\varphi}{\nu}\right)}{\sin\left(\dfrac{\pi - \delta + \varphi}{\nu}\right) - \sin\left(\dfrac{\delta - \varphi}{\nu}\right)} \qquad (11)$$

$$U'_{CM} = 2\frac{\sin\left(\dfrac{\varphi}{\nu}\right) + U'_0 \sin\left(\dfrac{\pi - \delta + \varphi}{\nu}\right)}{\sin\left(\dfrac{\pi}{\nu}\right)} - (1 + kU'_0) \qquad (12)$$

Now, after calculation of the U'_0 and U'_{CM} values, the other coefficients of the model – the initial values of the current i'L through the inductor and the voltage u'_C across the capacitor, can also be determined for the second and the third intervals. For this purpose, Eqs. (4) are used.

Analyzing the obtained dependencies, it can be observed that all the model coefficients are expressed by two angles. One of them is the control angle δ, which represents a parameter. The other angle is φ. Its value depends on the converter load. In other words, the model coefficients are determined in accordance with the value of the control parameter δ for a determined load expressed by the angle φ.

MODE	Angle δ	Angle φ
DIRECT	$0 \div \pi/2$	$0 \div \delta$
	$\pi/2 \div \pi$	$0 \div \pi/2$
REVERCE	$\pi \div 3\pi/2$	$\pi/2 \div \pi$
	$3\pi/2 \div 2\pi$	$\delta - \pi \div \pi$

Table 2

During the calculations, the limits of the angle φ variation must be taken into consideration. They depend on the operating mode, as well as, on the value of angle δ. The possible limits are presented in Table 2.
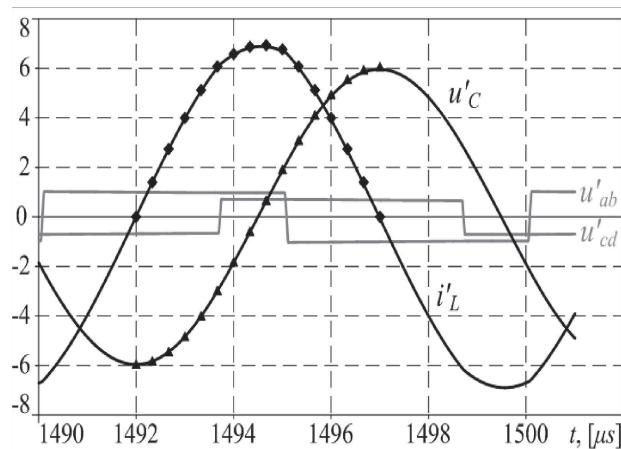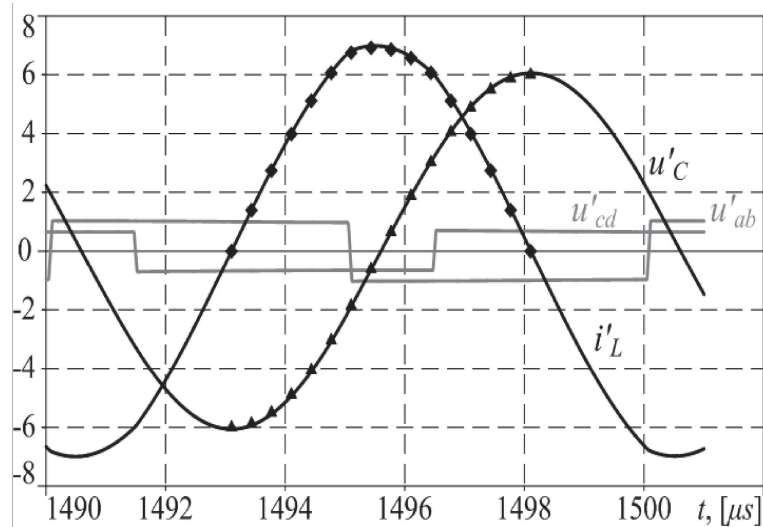

Figure 4. Comparison at DIRECT MODE

Figure 5. Comparison at REVERCE MODE

4. Reliability of the Results

For verification of their authenticity, the results from the accomplished modeling are compared to ones obtained from computer simulations. For this purpose, a model of a bidirectional series resonant DC-DC converter operating above the resonant frequency is realized in the environment of OrCAD PSpice. The simulation model has the following main parameters: Input source voltage – U_d = 200V; Resonant tank circuit inductance – L = 223,332μH; Resonant tank circuit capacitance – C = 15nF; Operating frequency – f_S = 100kHz; Frequency detuning – v =1,15; Transformation ratio k = 1.

The obtained simulation results are normalized in the same way as the values from the above presented modelling. Comparison in graphic form for the DIRECT MODE is presented in Figure 4, and for the REVERCE MODE – in Figure 5. The waveforms of the voltages u_{ab}, u_{cd}, u_C and the current i_L obtained from the computer simulations are shown with thick lines. The calculation results are presented by means of symbols (♦ – for the current i_L and ▲ – for the voltage uC). The examinations for the DIRECT MODE are accomplished at δ = 0,722π and φ = 0,389π (U'_0 = 0,67972), and for the REVERCE MODE – δ = 1,278π and φ = 0,611π (U'0 = 0,67972).

A very good coincidence between the results obtained from the simulations and from the calculations is observed from the charts. This is also confirmed by the accomplished examinations for other converter operating points.

5. Conclusion

A modelling of the resonant tank circuit processes of bidirectional series resonant DC-DC converter operating above the resonant frequency is executed. For this purposes, well-known analytical models are used with their coefficients being determined for the considered circuit. Computer simulations are accomplished, the results ofwhich show very good coincidence with those from the analytical modelling.

The obtained models can be used for future investigation and design of such converters.

References

[1] Cheron, Y., Foch, H., Roux, J. (1986). Power Transfer Control Methods in High Frequency Resonant Converters, *PCI Proceedings*, Munich, June, 92-103.

[2] Alhaddad, K., Cheron, Y., Foch, H., Rajagopalan, V. (1986). Static and Dynamic Analysis of a Series-Resonant Converter

Operating above its Resonant Frequency, *PCI Proceedings*, Boston, October 1986, 55-68.

[3] Patent ! 4717990, U.S. H04M 7/00; H02J 3/38: Cheron Y., P. Jacob, J. Salesse; Static Device for Control of Energy- Exchange between Electrical Generating and/or Receiving Systems, January 1988.

[4] Dixneuf Daniel. (1988). Etud d'un variateur de vitesse a resonance pour machine asynchrone triphasee, These, 1988.

[5] Chan, H.L., Cheng, K.W.E., Sutanto, D. (1999). A Fhase-Shift Controlled Bi-directional DC-DC Converter, *42nd Midwest Symposium on Circuits and Systems*, Volume 2, 723-726.

[6] Jalbrzykowski, S., Citko, T. (2009). A bidirectional DC-DC converter for renewable energy systems, *Bulletin of the Polish Academy of Sciences, Technical Sciences*, 57 (4) 363-368.

[7] Ramya, K., Sundaramoorthi, R. (2014). Bidirectional Power Flow Control using CLLC Resonant Converter for DC Distribution System, *International Journal of Advanced Research in Electrical*, *Electronics and Instrumentation Engineering*, 3 (4) 8716-8725, April 2014, ISSN: 2278 – 8875.

[8] Ancy, A.M, Arjun, Siby C. (2014). A Resonant Converter Topology for Bidirectional DC DC Converter, *International Journal of Engineering Research & Technology*, 3 (9) 469- 473, September, ISSN: 2278-0181.

[9] Dharuman, D., Thulasiyammal, C. (2014). Power Flow Control Using Bidirectional Dc/Dc Converter for Grid Connected Photovoltaic Power System, *International Journal of Innovative Research in Electronics and Communications*, 1 (8) 13-24, November 2014, ISSN 2349-4050.

[10] Jang, Y., Jovanovi, M. M., Ruiz, J. M., Liu, G. (2015). Series-Resonant Converter with Reduced-Frequency-Range Control, *Applied Power Electronics Conference and Exposition (APEC)*, 2015 IEEE, 1453-1460, 15-19 March 2015, Charlotte, NC.